

아연-프탈로시아닌에 의한 탄소나노튜브의 비공유 기능화와 이를 포함하는 폴리불화비닐리덴의 베타상 형성에 대한 연구

손호승 · 이재훈* · 정종한 · 한성훈 · 고중혁* · 박종승[†]

부산대학교 유기소재시스템공학과, *중앙대학교 전기전자공학부
(2020년 1월 21일 접수, 2020년 3월 16일 수정, 2020년 3월 16일 채택)

Noncovalent Functionalization of Single-walled Carbon Nanotubes Using Alkylated Zinc-phthalocyanine for the β -phase Formation of a Polyvinylidene Fluoride Matrix

Hoseung Son, Jae-Hoon Ji*, Jong Han Jeong, Seong-Hoon Han, Jung-Hyuk Koh*, and Jong S. Park[†]

Department of Organic Material Science and Engineering, Pusan National University, Busan 46241, Korea

*School of Electrical and Electronics Engineering, Chung-Ang University, Seoul 06974, Korea

(Received January 21, 2020; Revised March 16, 2020; Accepted March 16, 2020)

초록: 본 논문에서는 알킬기를 가지는 아연-프탈로시아닌(R-ZnPc)을 이용하여 단일벽 탄소나노튜브(single-walled carbon nanotube, SWCNT)의 분산 특성을 파악하고 이를 포함하는 폴리불화비닐리덴(polyvinylidene fluoride, PVDF)의 베타상(β -phase) 형성에 대한 연구 결과를 제시한다. R-ZnPc는 알킬기를 가지는 프탈로니트릴(phthalonitrile) 중간체를 아연염과 함께 tetramerization 반응을 진행하여 합성하였다. 긴 알킬기가 외부에 존재하기 때문에 R-ZnPc는 다양한 유기 용매에 높은 용해성을 발휘하였다. 또한 알킬기의 소수성 상호작용과 편평한 분자구조의 특징을 이용하여 SWCNT 외벽에 R-ZnPc 분자 wrapping을 유도하여 비공유 결합에 기반한 초분자 복합체(supra-molecular complex)를 제조하였다. Pc-CNT 복합체를 자외-가시광 흡수도, 푸리에 적외선 분광법, 라만 분광법, 열중량 분석법, 주사전자현미경 측정 및 X선 광전자 분광법 등 다양한 측정 방법으로 분석하였다. 또한 Pc-CNT 복합체를 나노필러로 사용하여 Pc-CNT/PVDF 복합 필름(composite film)을 제조하였다. Pc-CNT/PVDF 복합 필름의 유전 상수는 큰 폭으로 증가하였으며 이는 PVDF의 베타상 형성이 촉진되었기 때문인 것으로 푸리에 적외선 분광법과 X선 회절분석법 측정을 통해 확인하였다. 본 연구 결과는 R-ZnPc가 SWCNT 표면을 효과적으로 기능화할 수 있으며 제조된 Pc-CNT 복합체가 PVDF 매트릭스의 결정 구조 변화에 영향을 미쳤다는 것을 의미한다. 또한 본 연구에서 제시하는 방법은 하이브리드 복합 필름에 적합한 나노필러를 제조하는데 유용한 방법이 될 것으로 기대된다.

Abstract: We present the dispersion properties of alkylated zinc-phthalocyanine (R-ZnPc) for single-walled carbon nanotubes (SWCNTs), which finds useful for the β -phase formation of a polyvinylidene fluoride (PVDF) matrix. The R-ZnPc was prepared by direct tetramerization of alkylated phthalonitrile with zinc salts. Due to the presence of long peripheral alkyl-substituents, the prepared R-ZnPc exhibited controllable solubility in selected solvents. Taking advantage of the hydrophobic interactions of alkyl chains and flat structural features of Pc macrocycles, molecular wrapping of R-ZnPc around the SWCNTs was intended to produce noncovalent supramolecular complexes. The prepared Pc-CNT complexes were analyzed by various characterization methods, including UV-Vis, FTIR, Raman, TGA, SEM, and XPS measurements. Furthermore, the Pc-CNT/PVDF composite films were prepared using the Pc-CNT complex as effective nano-fillers for the PVDF matrix. The dielectric constants of the Pc-CNT/PVDF composite films were significantly increased as a consequence of the promoted β -phase formation in the PVDF matrix, as evidenced by FTIR and XRD measurements. Current results suggested that the R-ZnPc functionalized SWCNTs have affected the crystalline structure of the PVDF matrix, which can be a useful tool for producing nano-fillers for hybrid polymer composites.

Keywords: polyvinylidene fluoride, zinc-phthalocyanine, single-walled carbon nanotube, carbon nanotube, composite, dielectric constant.

[†]To whom correspondence should be addressed.
jongpark@pusan.ac.kr, ORCID[®]0000-0002-7624-9502
©2020 The Polymer Society of Korea. All rights reserved.

Introduction

Polyvinylidene fluoride (PVDF) and its copolymers have been widely used in many application fields because of their superior piezoelectric, ferroelectric properties and dielectric constants.¹⁻⁴ The electrical properties were closely related to various semi-crystalline polymorphs of PVDF.^{5,6} Among semi-crystalline phases, β -phase showed outstanding electrical properties owing to its all-trans (TTT) configuration.^{7,8} The experimental techniques and strategies to induce the β -phase structure have been investigated in particular conditions, such as drawing films, applying an extremely high electric field, and crystallization from a solution or melt.^{9,10}

As a measure to enhance the electrical properties of PVDF and facilitate the β -phase formation, the polymer nanocomposites combined with inorganic nano-fillers have been widely investigated.¹¹⁻¹³ Inorganic fillers, such as BaTiO₃, Ti₄O₁₂, and Pb(Zr,Ti)O₃, have been combined with PVDF, which effectively enhanced the physical, mechanical and electrical properties.¹⁴⁻¹⁷ However, these nanocomposites with inorganic fillers created processing problems because these fillers made PVDF significantly dense and brittle. Meanwhile, organic fillers are useful in maintaining the flexibility of PVDF nanocomposites. Notably, carbon nanotubes (CNTs) have been extensively investigated because of their electrical properties, low mass density, and large aspect ratio, which effectively enhanced the electrical, ferroelectric, and piezoelectric properties of the PVDF composites.¹⁸⁻²² However, since CNTs are tightly entangled with each other by secure van der Waals forces, appropriate surface treatment and pre-milling procedures needed to be applied to distribute CNTs uniformly inside the PVDF matrix.

In order to disperse CNT bundles effectively inside the polymer matrix, numerous surface modification methods have been employed. Covalent functionalization of CNTs with a polymer matrix was tried, and, in this case, the polymer covering on the CNT surface provided adhesion and dispersion to the polymer matrix so that the prepared polymer composites had enhanced electrical and mechanical performances.²³⁻²⁵ However, the covalent approach mostly disrupted the well-ordered π -conjugated system and deteriorated the electrical and mechanical properties of the CNTs. To overcome the destruction of the structural nature, the non-covalent approach, which is weak and long-range interactions, can be used to maintain the inherent properties of CNTs. Among various methods, we have been especially intrigued by noncovalent functionalization

with metallophthalocyanines (MPcs).²⁶ Due to excellent chemical, thermal, and light stability, the polymer composites including MPc have provided high electrical conductivity and superior mechanical and chemical stability, along with superb electrochemical activities.²⁷⁻²⁹

Meanwhile, several polymers have been employed as matrix materials for preparing polymer-based nanocomposites.³⁰⁻³³ PVDF and its copolymers have exhibited relatively high dielectric permittivity and breakdown strength, compared to other commodity polymers. However, despite many approaches, the dielectric constant values are still low, and thus the practical applications for energy storage capacitors are quite limited.

In this article we present the preparation and applications of alkylated zinc-phthalocyanine (R-ZnPc) for noncovalent functionalization of single-walled carbon nanotubes (SWCNTs), which we then use as a nanofiller for PVDF composites. Peripherally substituted ZnPcs are suitable for SWCNT modification due to hydrophobic interactions of alkyl chains and flat molecular structure of the Pc macrocycles. Furthermore, alkyl chains at peripheral sites of ZnPc allowed the molecular wrapping of Pcs around the SWCNTs. Thus, we expected that a large amount of ZnPcs would firmly adhere to the CNTs surface and that the enhanced compatibility would increase the dispersing nature of the SWCNTs inside the PVDF polymer matrix. Furthermore, Pc-functionalized SWCNTs affected the crystalline structure of the PVDF, inducing more β -phase during nucleation inside the matrix. The prepared ZnPc and Pc-CNT complex was fully examined using various characterization methods. The effect of the Pc-CNT filler on the β -phase formation of the polymer matrix was examined, and the resulting dielectric properties of ZnPc-CNT/PVDF composite film were presented.

Experimental

Chemicals. Lithium metal, zinc(II) acetate, 1-hexanol, 1,8-diazabicyclo[5.4.0]undec-7-ene, polyvinylidene fluoride (PVDF), tetrahydrofuran (THF), dichloromethane (DCM), and *N,N*-dimethylacetamide (DMAc) were purchased from Sigma-Aldrich. 4-Nitrophthalonitrile was purchased from TCI, and vinyl terminated polyisobutylene (HRPB1000) was provided by Daelim Corporation (Korea). All reagents were used without further purification. SWCNTs (>90 wt%, diameter 1.1 nm, length 1-3 μ m) were purchased from US Research Nanomaterials.

Synthetic Procedures. Synthesis of Alkylated Phthalonitrile: PIB1000-alcohol was synthesized by following the pre-

vious literature procedure.³⁴ A mixture of 4-nitrophthalonitrile (1.63 g, 8.89 mmol), PIB1000-alcohol (3.0 g, 2.96 mmol), and Cs_2CO_3 (4.81 g, 14.81 mmol) was dissolved in 30 mL of THF and refluxed in the inert gas for 12 h. The residue was cooled to room temperature, and the THF was evaporated under reduced pressure. The crude products was extracted with hexane, and washed with a 90% ethanol-water mixture three times, then dried over MgSO_4 . Hexane was removed under reduced pressure using a rotary evaporator to afford alkylated phthalonitrile as a viscous oil (2.89 g, 85.3% yield). ^1H NMR (500 MHz, CDCl_3) δ 7.69 (d, $J=8.5$ Hz, 1H), 7.24 (d, $J=2.0$ Hz, 1H), 7.16 (dd, $J=8.5, 2.10$ Hz, 1H), 3.85 (dd, $J=8.5, 5.5$ Hz, 1H), 3.74–3.71 (m, 1H), 1.61–0.85 (multiple peaks). MALDI-Mass ($\text{C}_{79}\text{H}_{148}\text{N}_2\text{O}$) 1131.18 m/z.

Synthesis of Alkylated Zinc-phthalocyanine (R-ZnPc): Alkylated phthalonitrile (1 g, 0.877 mmol) and ZnCl_2 (44 mg, 0.323 mmol) were added to the pressure tube, and the reaction mixture was heated to 160 °C for 4 h. After cooled down to 25 °C. The alkylated zinc-phthalocyanine was extracted with hexane and washed with acetonitrile and a 90% ethanol-water mixture three times. After being dried over MgSO_4 , then filtered, hexane was removed under reduced pressure. The alkylated zinc-phthalocyanine was isolated by column chromatography using silica gel and (DCM/hexane 4:6) as the eluent, and the product was a greenish viscous oil. ^1H NMR (500 MHz, CDCl_3) δ 9.05 (s, 3H), 8.54 (d, $J=58.7$ Hz, 4H), 7.62 (s, 5H), 4.39–4.22 (m, 8H), 2.50–0.70 (multiple peaks). MALDI-mass ($\text{C}_{316}\text{H}_{584}\text{N}_8\text{O}_4\text{Zn}$) 4620 m/z.

Preparation of the Pc-CNT Complex: 1 mg SWCNT was sonicated in 10 mL CHCl_3 for 30 min at 0 °C in a sonication bath (PowerSonic410, Hwashin, Korea). A solution of R-ZnPc 2 mg in 1 mL of CHCl_3 was added dropwise to the above SWCNT solution, and the mixed solution additionally was sonicated for 1 h. The resulting ZnPc/SWCNT complex was isolated with a PTFE membrane filter (pore size 200 nm). The residue was washed successively with CHCl_3 to remove excess ZnPc and proceed until the filtrate was colorless. The complex was collected and dried in a vacuum oven for 24 h.

Preparation of the Pc-CNT/PVDF Composite: 1 g of PVDF in 5 mL of DMAc was stirred at 50 °C until a homogeneous solution was obtained. Meanwhile, the Pc-CNT dispersion in 1 mL DMAc was prepared by sonication of the solution for 30 min at 0 °C in a sonication bath (PowerSonic410, Hwashin, Korea). Then, the PVDF solution and Pc-CNT dispersion were mixed in the desired quantity to make a suspension by sonication for 30 min. The suspensions were

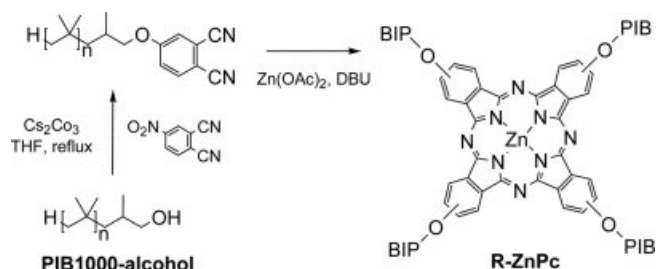
coated on a glass plate by the doctor blade method, and the film thickness was controlled to 0.5 mm and dried in a vacuum oven at 80 °C.

Property Characterization: ^1H NMR measurements were performed on an Inova Tech at 500 MHz using CDCl_3 as a solvent. The UV-Vis absorption and photoluminescence spectra were measured by using Shimadzu UV-1800 spectrophotometer and Perkin-Elmer LS-45 spectrofluorometer, respectively. MALDI-TOF mass spectrometry, X-ray photoelectron spectroscopy, and FTIR analysis were measured at the Korea Basic Science Institute. Thermogravimetric analysis (TGA, STA6000, Perkin-Elmer) was performed in nitrogen at a heating rate of 10 °C/min. Field emission scanning electron microscopy (FE-SEM) was performed on a SUPRA25 (Carl Zeiss AG, Germany). Raman spectra were measured using a NRS-5100 with an excitation laser of 532 nm. X-ray diffraction (XRD) analysis was analyzed using Xpert 3. The dielectric constant and dielectric loss values obtained on a HP 4194A impedance analyzer at room temperature in the frequency range of 60 Hz to 10 MHz.

Results and Discussion

The alkylated phthalonitrile, an intermediate, was synthesized by refluxing the hydroxy-terminated polyisobutylene with 4-nitrophthalonitrile in the presence of Cs_2CO_3 . The cyclotetramerization of alkylated phthalonitrile with zinc(II) chloride produced alkylated zinc phthalocyanine (R-ZnPc). (Scheme 1). The structure of R-ZnPc product was successfully identified by MALDI-Mass spectroscopy.

Generally, in UV-Vis spectra, Pc compounds have two absorption characteristics, one in the UV region (B- or Soret band) and the other in the visible region (Q-band).³⁵ As shown in Figure 1, R-ZnPc exhibited a sharp Q-band at 683 nm. R-ZnPc became highly soluble in THF and chloroform, but only a small amount was soluble in nonpolar solvents like hexane.



Scheme 1. Synthesis of alkylated zinc phthalocyanines (R-ZnPc).

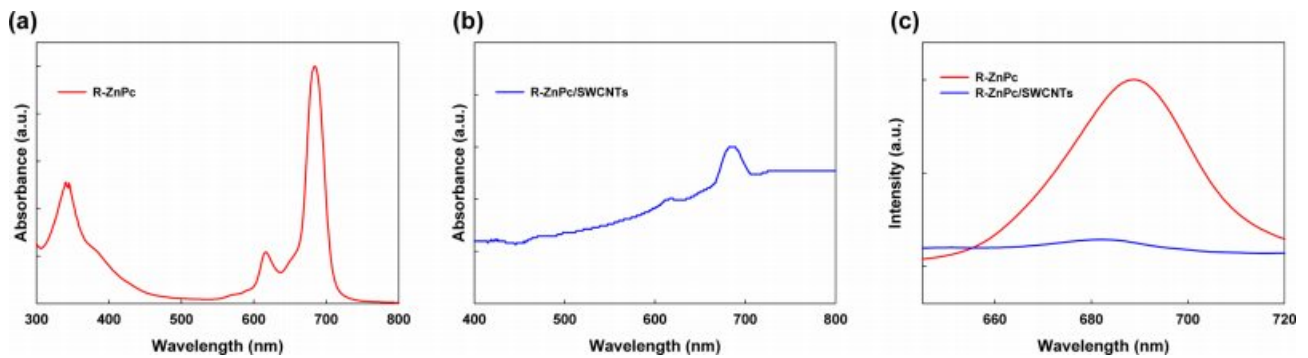


Figure 1. UV spectra of (a) R-ZnPc; (b) Pc-CNT complex in dichloromethane. (c) Corresponding emission spectra of R-ZnPc and Pc-CNT complex in dichloromethane.

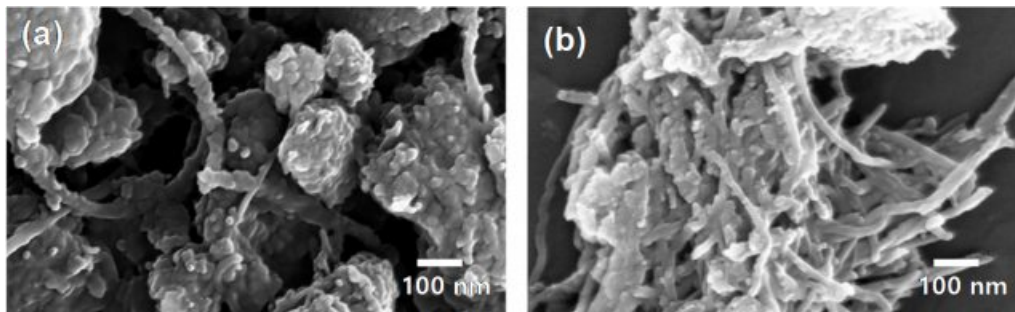


Figure 2. SEM images of (a) pristine SWCNTs; (b) the Pc-CNT complex.

The Pc-CNT complex was prepared by sonication of R-ZnPc and SWCNTs in chloroform for 1 h. Due to long, multiple peripheral chains and the flat molecular structure of the phthalocyanine skeleton, the R-ZnPc exhibited high affinity and strong adhesion to the surface of the SWCNTs. The UV-Vis spectra of Pc-CNT complexes revealed significant absorption and scattering effect of CNT bundles in the range of 300 and 600 nm. The Q-band of R-ZnPc in the Pc-CNT complex was also observed at 689 nm, with a slight red shift by 6 nm. This red shift in the Q-band after complex formation is evidence of the existing noncovalent interaction of ZnPcs with SWCNTs. In PL spectra, R-ZnPc exhibited the emission maximum at 689 nm with excitation at 600 nm. After the complex formation, the PL intensity was quenched entirely as a result of a facile electron transfer from ZnPc to SWCNT in the formed complex.

The morphological difference between pristine and ZnPc-functionalized SWCNTs was noticed in the SEM images (Figure 2). In pristine SWCNTs, the CNT bundles randomly adhered to each other, forming irregular aggregates. After the complex formed, the surface of Pc-CNT complexes was mostly separated into individual CNTs. Therefore, R-ZnPc

induced the presence of individual tubes as a result of effective de-bundling on the CNT surface.

In the FTIR analysis, a strong absorption band with a C=C stretch of SWCNTs was observed at around 1600 cm^{-1} and a slight red shift at high frequencies after being complexed. It was attributed to intramolecular electron transfer between non-covalently bonded Pc-CNT complexes (Figure 3(a)). Compared to the featureless spectrum of pristine SWCNTs, the Pc-CNT complex exhibited characteristic peaks of the pyrrole backbone in the range of $1550\text{--}1200\text{ cm}^{-1}$. The characteristic absorption in the aromatic region of CNTs almost disappeared due to the appearance of aliphatic peaks in the Pc-CNT complex (about $2900\text{--}2800\text{ cm}^{-1}$). This result indicated that the polyisobutylene substituent completely wrapped the aromatic structure of CNT surface (Figure 3(b)).

To investigate the structural features of the functionalized SWCNTs with R-ZnPc, Raman spectroscopy was employed. The Raman spectrum of pristine SWCNTs represented a broad D-band peak at 1335 cm^{-1} , attributed to the vibrations of sp^3 -hybridized carbon structures, and a G-band peak at 1580 cm^{-1} , attributed to in-plane vibration of sp^2 -hybridized graphitic carbon atoms,^{35,36} yielding an I_D/I_G ratio of 0.46 (Figure 4(a)). After

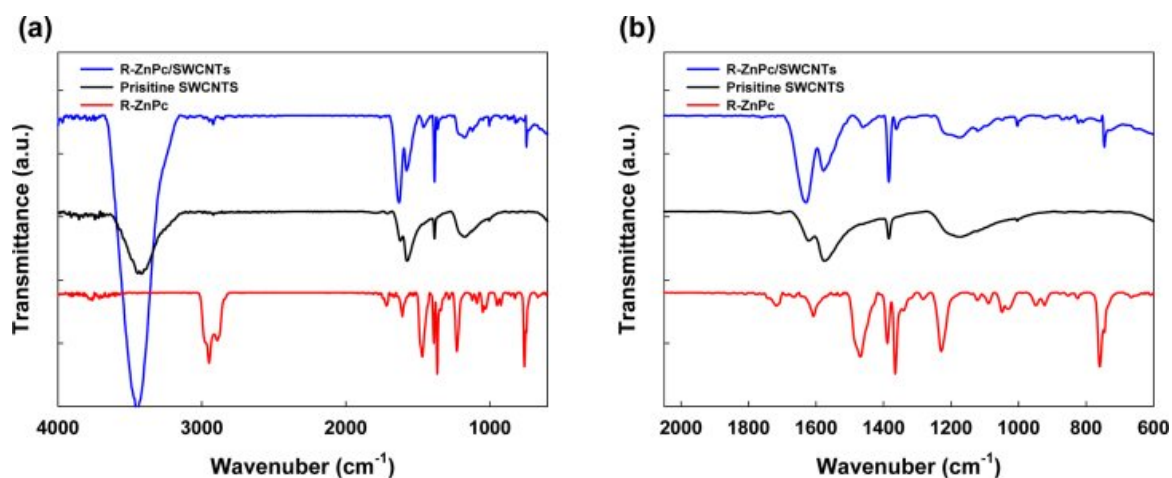


Figure 3. (a) FTIR spectra of R-ZnPc, the Pc-CNT complex, and pristine SWCNTs; (b) magnified spectra in the range from 600 to 2000 cm^{-1} of the corresponding samples.

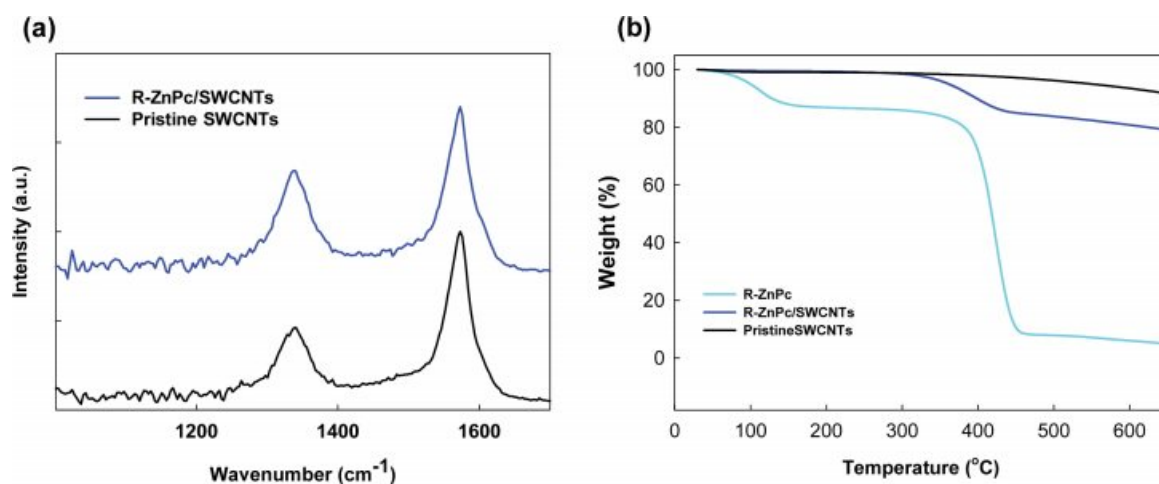


Figure 4. (a) Raman spectra of Pc-CNT complexes; (b) TGA thermograms of R-ZnPc and Pc-CNT complexes.

the CNT is functionalized with R-ZnPc, the D- and G-bands of the complex shift slightly to higher frequencies, indicating the extended electron delocalization. As a result, the I_D/I_G ratio of the Pc-CNT complex increased significantly to 0.68. TGA measurements were performed to analyze the thermal stability of the prepared complexes and to estimate the amount of Pc stacked on the SWCNTs by non-covalent bonding (Figure 4(b)). Over a wide temperature range, the pristine SWCNTs were stable, with only a 10% weight loss above 650 $^{\circ}\text{C}$, mainly due to the impurities included in the nanotube preparation.²⁸ R-ZnPc began to slowly degrade at 100–400 $^{\circ}\text{C}$ due to PIB chain breakage and showed a massive weight loss of about 400 $^{\circ}\text{C}$, which corresponds to complete decomposition of the Pc skeleton. The Pc-CNT complex showed degradation and weight-loss behavior due to the detachments of surface decorating

molecules.

XPS measurements were performed to analyze the ZnPc skeletons and polyisobutylene, the characteristics of ZnPc-CNT. The deconvolution of C_{1s} peaks indicated two primary carbon atoms, C-C and C-O at 284.6 and 285.6 eV, respectively (Figure 5(a)).^{37,38} The N_{1s} peak was deconvoluted into two separate 398.7 and 399.8 eV peaks, due to the pyridinic and pyrrolic nitrogens of phthalocyanine (Figure 5(b)). The Zn_{2p} peaks were deconvoluted into two peaks at 1021 and 1044 eV, corresponding to bond energy values of $\text{Zn}_{2p_{1/2}}$ and $\text{Zn}_{2p_{3/2}}$, respectively (Figure 5(c)).

The SEM images of the Pc-CNT/PVDF composite were prepared in a film state, which revealed smaller particles and fewer surface voids compared to pristine PVDF films (Figure 6(a) and 6(b)). Since the surface-modified SWCNTs were uni-

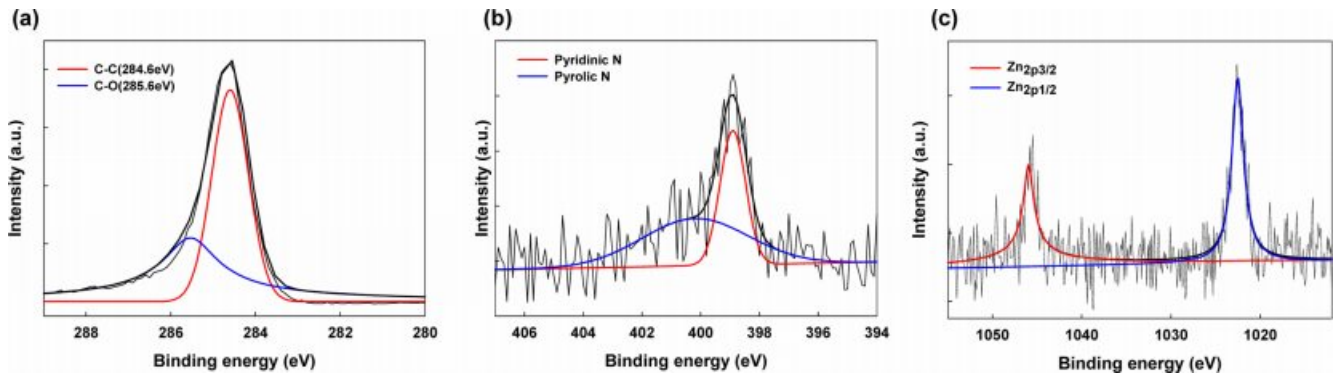


Figure 5. XPS C_{1s} spectra of Pc-CNT complexes; (b) XPS N_{1s} spectra of the Pc-CNT complexes; (c) deconvoluted Zn_{2p} XPS spectra of the Pc-CNT complexes.

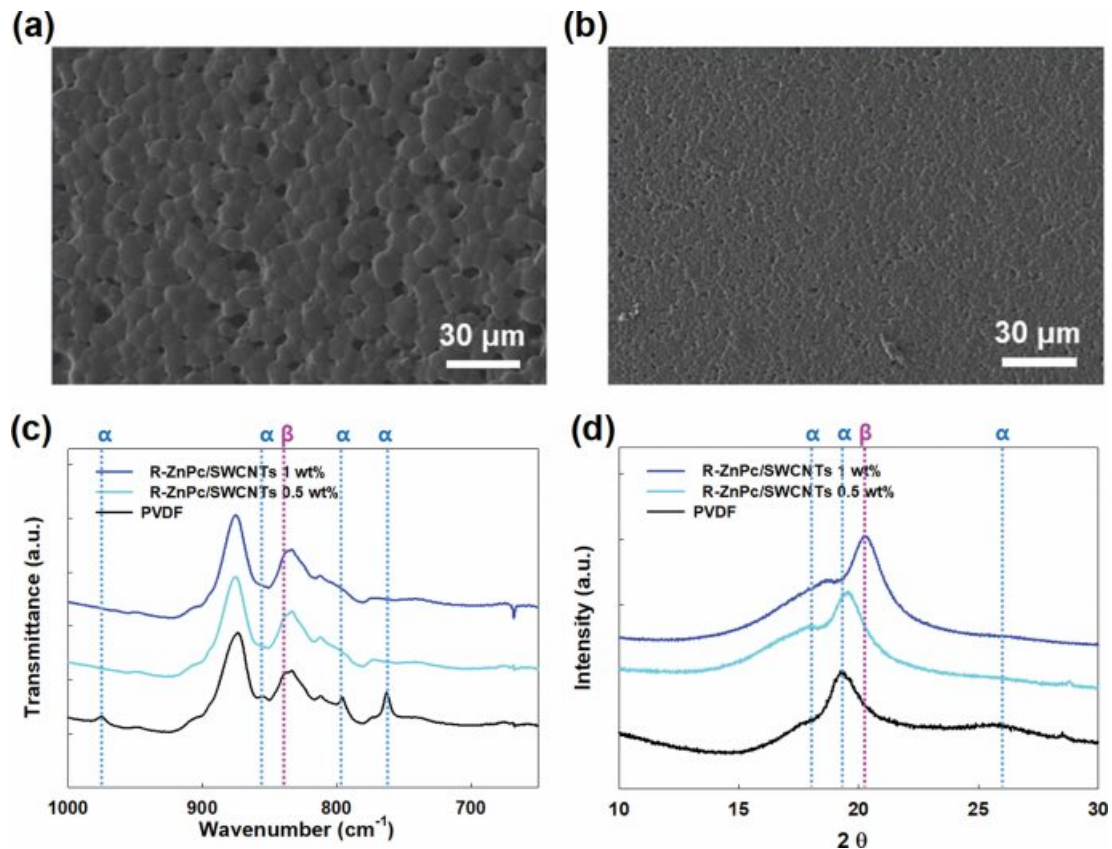


Figure 6. The surface morphology of (a) PVDF; (b) Pc-CNT/PVDF composite films. The concentrations of the fillers are 5 wt%. FTIR spectroscopy measurements showing the reduced α -phase with the addition of (c) the Pc-CNT complex. X-ray diffraction measurement showing the enhancement of the β -phase with the addition of (d) the Pc-CNT complex.

formly dispersed in PVDF, the morphology of the PVDF composite was retained according to the filler content.

PVDF with various semi-crystalline polymorphs have exhibited different molecular vibrations in FTIR spectroscopy. The absorption spectra at 613, 762, 795, and 975 cm^{-1} are the characteristic spectra for the α -phase crystalline, and the bands at

840 and 1275 cm^{-1} are assigned for β -phase crystalline.³⁹ In current measurements, the FTIR spectra were performed to analyze the crystalline phase of PVDF composites with different amounts of Pc-CNT. All these peaks were observed in the prepared PVDF films (Figure 6(c)), indicating that PVDF formed both α - and β -phases simultaneously during the crystal

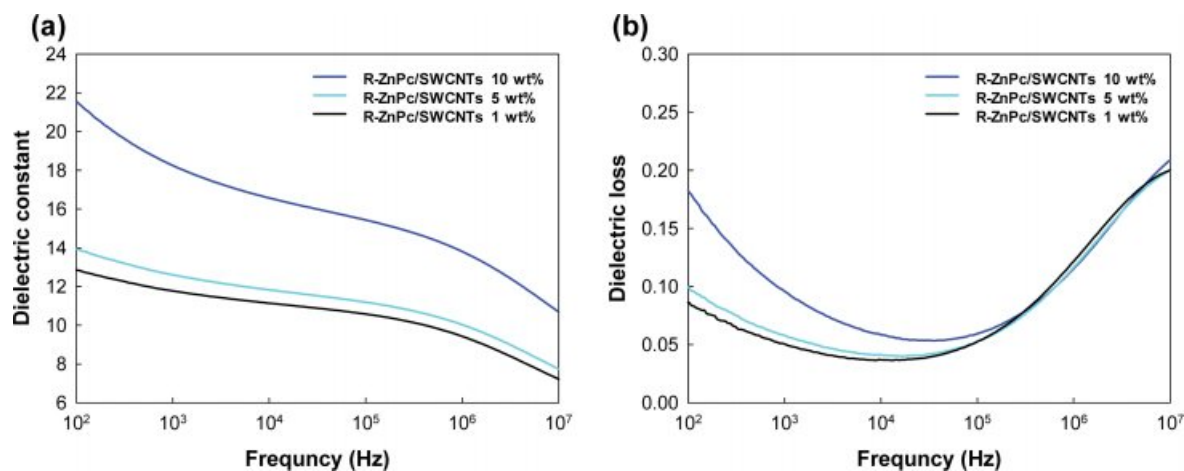


Figure 7. Dielectric constant (a) and dielectric loss (b) of PC-CNT/PVDF composite films with different concentrations of the Pc-CNT complex.

formation. However, when the content of R-ZnPc/SWCNTs was 0.5% in PVDF, the intensity of the α -phase showed a decreasing tendency.

The α - and β -phases in the PVDF matrix can also be distinguished through X-ray diffraction measurement (Figure 6(d)). Generally, the α -phase crystalline of PVDF exhibits strong diffraction peaks at $2\theta=17.8^\circ$ and 19.5° , respectively, assigned to the lattice planes of (100) and (110). The α -phase can also be observed at $2\theta=26^\circ$ corresponding to the (021) lattice plane. The peak at $2\theta=20.6^\circ$ is assigned to (110) and (200) planes in the β -phase crystalline.⁴⁰ The XRD pattern of PVDF clearly showed two sharp diffraction peaks at $2\theta=17.8^\circ$ and 19.5° , corresponding to α phase (020) and (110) planes, respectively, and one broad peak at $2\theta=26.8^\circ$ of the α phase (021). In the PVDF nanocomposite film, the 0.5% Pc-CNTs were not different from those of pristine PVDF. However, in the 1% Pc-CNTs, the intensity of the peaks at $2\theta=17.8^\circ$, 19.5° , and 26.8° was decreased and a new peak at $2\theta=19.5^\circ$ corresponding to the β -phase (for 110 and 200 planes) was formed with higher intensity. These results indicate that the functionalized CNTs dispersed well inside the PVDF matrix and promoted β -phase formation.

The dielectric constant was investigated over a wide range of frequencies from 100 Hz to 1 MHz for the Pc-CNT/PVDF composite (Figure 7). When the amount of Pc-CNT fillers was below 5 wt%, the change in the dielectric constant was small, showing a slight increase in low-frequency regions, resulting in low capacitance. When the fraction of the fillers increased to 10 wt%, the dielectric constant was significantly increased, which was attributed to the formation of sizable interfacial

polarization. The improvement of the dielectric constant with the amount of functionalized SWCNT filler is explained as a consequence of the promoted β -phase formation in the PVDF matrix,⁴¹⁻⁴³ as evidenced by FTIR and XRD measurements. Meanwhile, the dielectric loss of the Pc-CNT/PVDF composite films was also measured. Similarly, the low content of the Pc-CNT complex in PVDF did not alter the curve. In the case of the 10 wt% filler content, the dielectric loss value showed a slight increase in low-frequency regions. The behavior was attributed to the overlap of SWCNTs in the PVDF matrix, contributing to the formation of conductive networks. However, an extreme increment in the dielectric loss was not observed in the composite, while exhibiting the enhanced dielectric constant values. These results suggest that noncovalent functionalization using substituted metallophthalocyanines can be a practical method in producing nanofillers that are useful for enhancement in dielectric properties of PVDF based polymer composites.

Conclusions

We have synthesized alkylated zinc-phthalocyanine (R-ZnPc) by direct tetramerization of alkylated phthalonitrile with zinc salt. Taking advantage of preferential interactions of Pc macrocycles with single-walled carbon nanotube (SWCNT), we have produced supramolecular complexes from the molecular wrapping of R-ZnPc around SWCNTs. The prepared Pc-CNT complexes were analyzed by various characterization techniques, including UV-Vis, FTIR, Raman, TGA, SEM, and XPS measurements. Besides, the Pc-CNT/PVDF composite

films were prepared, and their dielectric properties were examined. The dielectric constants were observed to be significantly increased, which was due to the promoted β -phase formation in the PVDF matrix, as evidenced by FTIR and XRD measurements.

Acknowledgments: This work was supported by the Technology Innovation Program (10047756 and 10052838) funded by the Ministry of Trade, Industry, and Energy (MOTIE, Korea).

References

1. Y. Liu, G. Tian, Y. Wang, J. Lin, Q. Zhang, and H. F. Hofmann, *J. Intell. Mater. Syst. Struct.*, **20**, 575 (2009).
2. J. B. Arochiam, H. S. Son, S. H. Han, G. Balamurugan, Y. H. Kim, and J. S. Park, *ACS Appl. Energy Mater.*, **2**, 8416 (2019).
3. T. W. Son, J. H. Kim, W. M. Choi, F. F. Han, and O. K. Kwon, *Polym. Korea*, **35**, 130 (2011).
4. C. E. Chang, V. H. Tran, J. B. Wang, Y. K. Fuh, and L. W. Lin, *Nano Lett.*, **10**, 726 (2010).
5. Prateek, V. K. Thakur, and R. K. Gupta, *Chem. Rev.*, **116**, 4260 (2016).
6. E. Ozkazanc and H. Y. Guney, *J. Appl. Polym. Sci.*, **112**, 2482 (2009).
7. L. David, J. I. Winsor, and B. Scheinbeim, *J. Polym. Sci., Part B: Polym. Phys.*, **34**, 2967 (1996).
8. P. Sukitpaneenit and T. S. Chung, *J. Membr. Sci.*, **340**, 192 (2009).
9. A. J. Lovinger, *Polymer*, **22**, 412 (1981).
10. H. Rekik, Z. Ghallabi, I. Royaud, M. Arous, G. Seytre, G. Boiteux, and A. Kallel, *Compos. Part B-Eng.*, **45**, 1199 (2013).
11. P. Martins, A. C. Lopes, and S. Lanceros-Mendez, *Prog. Polym. Sci.*, **39**, 683 (2014).
12. M. Arbatti, X. Shan, and Z. Cheng, *Adv. Mater.*, **19**, 1369 (2007).
13. P. Thomas, S. Satapathy, K. Dwarakanath, and K. B. R. Varma, *Polym. Lett.*, **4**, 621 (2010).
14. Z. H. Mbhele, M. G. Salemane, C. G. C. E. van Sittert, J. M. Nedeljkovic, V. Djokovic, and A. S. Luyt, *Chem. Mater.*, **15**, 5019 (2003).
15. I. Hussain, M. Brust, A. J. Papworth, and A. I. Cooper, *Langmuir*, **19**, 4831 (2003).
16. G. A. Gaddy, J. L. McLain, A. S. Korchev, B. L. Slaten, and G. Mills, *J. Phys. Chem. B*, **108**, 14858 (2004).
17. H. D. Yoon, S. Nam, N. D. K. Tu, D. Kim, and H. Kim, *Polym. Korea*, **37**, 638 (2013).
18. R. H. Baughman, A. A. Zakhidov, and W. A. Heer, *Science*, **297**, 787 (2002).
19. B. K. Kuila, S. Malik, S. K. Batabyal, and A. K. Nandi, *Macromolecules*, **40**, 278 (2007).
20. F. R. Fan, W. Tang, and Z. L. Wang, *Adv. Mater.*, **28**, 4283 (2016).
21. J. Eom, Y. R. Lee, J. H. Lee, S. K. Park, J. S. Park, and Y. H. Kim, *Compos. Sci. Technol.*, **169**, 1 (2019).
22. Y. R. Lee, J. Park, Y. Jeong, and J. S. Park, *Fiber. Polym.*, **19**, 2478 (2018).
23. P. Miaudet, C. Bartholome, A. Derre, M. Maugey, G. Sigaud, C. Zakri, and P. Poulin, *Polymer*, **48**, 4068 (2007).
24. R. Sen, B. Zhao, D. Perea, M. E. Itkis, H. Hu, J. Love, E. Bekyarova, and R. C. Haddon, *Nano Lett.*, **4**, 459 (2004).
25. H. H. Lee, U. S. Shin, G. Z. Jin, and H. W. Kim, *Bull. Korean Chem. Soc.*, **32**, 157 (2011).
26. H. S. Son, M. H. Yang, A. K. Mutyala, D. W. Chang, and J. S. Park, *Dyes Pigments*, **162**, 662 (2019).
27. A. Ndiaye, P. Bonnet, A. Pauly, M. Dubois, J. Brunet, C. Varenne, K. Guerin, and B. Lauron, *J. Phys. Chem. C*, **117**, 20217 (2013).
28. M. Li, X. Bo, Y. Zhang, C. Han, and L. Guo, *J. Power Sources*, **264**, 114 (2014).
29. P. J. Wei, G. Q. Yu, Y. Naruta, and J. G. Liu, *Angew. Chem. Int. Ed.*, **53**, 6659 (2014).
30. X. W. Liang, X. C. Yu, L. L. Lv, T. Zhao, S. B. Luo, S. H. Yu, R. Sun, C. P. Wong, and P. L. Zhu, *Nano Energy*, **68**, 104351 (2020).
31. K. Meeporn and P. Thongbai, *Compos. Part B-Eng.*, **184**, 107738 (2020).
32. L. Y. Xie, X. Y. Huang, Y. H. Huang, K. Yang, and P. K. Jiang, *J. Phys. Chem. C*, **117**, 22525 (2013).
33. L. M. Clayton, A. K. Sikder, A. Kumar, M. Cinke, M. Meyyappan, T. G. Gerasimov, and J. P. Harmon, *Adv. Funct. Mater.*, **15**, 101 (2005).
34. J. Li, S. Sung, J. Tian, and D. E. Bergbreiter, *Tetrahedron*, **61**, 12081 (2005).
35. A. Shaabani, R. Maleki-Moghaddam, A. Maleki, and A. H. Rezayan, *Dyes Pigments*, **74**, 279 (2007).
36. Y. Jiang, Y. Lu, X. Lv, D. Han, O. Zhang, L. Niu, and W. Chen, *ACS Catal.*, **3**, 1263 (2013).
37. C. Yang, S.-J. Hao, S.-L. Dai, and X.-Y. Zhang, *Carbon*, **117**, 301e312 (2017).
38. B. Wang, Y. Wu, X. Wang, Z. Chen, and C. He, *Sensor. Actuat. B-Chem.*, **190**, 157 (2014).
39. Y. Wang, A. D. Zhou, Y. Jiang, X. Y. Chen, and J. B. He, *RSC Adv.*, **5**, 37823 (2015).
40. S. X. Song, S. Xia, S. K. Jiang, X. Lv, S. L. Sun, and Q. M. Li, *Materials*, **11**, 347 (2018).
41. J. M. Zhu, X. Y. Ji, M. Yin, S. Y. Guo, and J. B. Shen, *Compos. Sci. Technol.*, **144**, 79 (2017).
42. R. Costa, J. Silva, and S. L. Mendez, *Compos. Part B-Eng.*, **93**, 310 (2016).
43. Y. H. Zhang, D. Xu, W. H. Xu, W. W. Wei, S. W. Guan, and Z. H. Jiang, *Compos. Sci. Technol.*, **104**, 89 (2014).